Environ. Sci. Technol. **1998**, *32,* 2051−2060

Gas-Phase and Particle-Phase Organic Compounds Emitted from Motor Vehicle Traffic in a Los Angeles Roadway Tunnel

MATTHEW P. FRASER,[†,‡] GLEN R. CASS,[*,†] AND BERND R. T. SIMONEIT[§]

Environmental Engineering Science Department, California Institute of Technology, Pasadena, California 91125, and College of Oceanic and Atmospheric Sciences, Oregon State University, Corvallis, Oregon 97331

The emission rates for 221 vapor-phase, semivolatile, and particle-phase organic compounds from motor vehicles plus fine particulate matter mass and some inorganic particle-phase species are calculated based on measurements made inside and outside a Los Angeles roadway tunnel in 1993. These emission rates are calculated based on fuel consumption to remove any uncertainties based on tunnel dilution rates or air circulation. The results show carbon monoxide emissions rates of 130 g L^{-1} of gasoline-equivalent fuel burned and volatile organic compound (VOC) emissions of 9.1 g L^{-1}. These values are higher than predicted by the baseline version of California's EMFAC 7G emissions inventory program but are within the coemission rate range of 108 ± 25 g L^{-1} reported by roadside remote sensing studies in Los Angeles [Singer, B. C.; Harley, R. A. *J. Air Waste Manage. Assoc.* **1996**, *46*, 581−593]. When the VOC emissions composition in the tunnel is compared to that of tailpipe emissions source test data and to the composition of additional unburned whole gasoline, the tunnel atmosphere is found to be consistent with a linear combination of these major contributors over a fairly broad range of about 74−97% vehicle exhaust depending on the tailpipe profiles used. Fine particulate emissions within the tunnel consist largely of carbonaceous material accompanied by a significant amount of ammonium nitrate apparently formed by gas-to-particle conversion processes within the tunnel atmosphere. Certain gas-phase and particulate organic compounds traditionally thought to be the secondary products of atmospheric chemical reactions are enriched inside the tunnel, and from this enrichment, the primary emission rates of aromatic alcohols, aliphatic dicarboxylic acids, and aromatic polycarboxylic acids are calculated. Data on petroleum biomarkers emissions rates in the tunnel can be used in the future to estimate primary vehicle exhaust fine particulate matter concentrations in the urban atmosphere.

* To whom correspondence should be addressed. Phone: (626)-395-6888; fax: (626)395-2940; e-mail: glen@eql.caltech.edu.

† California Institute of Technology.

‡ Current address: Department of Environmental Science and Engineeering, Rice University, Houston, TX 77005.

§ Oregon State University.

Introduction

To understand the contribution of motor vehicles to air pollution, accurate characterization of vehicular emissions is needed. Ideally, this characterization should reflect the vehicle emissions as they occur under actual operation on the highway. Furthermore, the chemical complexity of these emissions should be fully described. Conventional emissions inventories that state the volatile organic compound (VOC) and particulate matter (PM) emissions from vehicles often provide only a lumped representation of the hundreds of organic compounds that are actually present in vehicular emissions. Individual VOCs can have dramatically different chemical reactivity with respect to ozone formation (*2*), while some VOCs (e.g., formaldehyde and benzene) are toxic air contaminants, as are certain particle-phase species (e.g., specific polycyclic aromatic hydrocarbons) (*3*). Other specific VOCs (e.g., many aromatics) are secondary aerosol precursors (*4*), and with the exception of a few studies (e.g., refs *5*−*7*), semivolatile organics in the molecular weight range above C_{10} or C_{12} are seldom measured at all.

The purpose of this paper is to report a comprehensive characterization of the individual organic species emitted from motor vehicles. Individual vapor-phase, semivolatile, and particle-phase organics are characterized simultaneously over the range of molecular weights from C_1 to C_{33}. Measurements are made of the emissions from over 7000 motor vehicles under actual operation on a Los Angeles area surface street as they pass through a highway tunnel. This experiment was conducted in conjunction with a comprehensive characterization of VOC, semivolatile, and particle-phase organic compounds in Los Angeles ambient air in order to provide model evaluation data for use in testing photochemical airshed models that simultaneously track both gas-phase and particle-phase organic compounds (*8*−*12*).

Measurements made in Los Angeles are of particular importance. The Los Angeles area experiences the nation's worst photochemical smog problem and highest fine particle concentrations (*13*, *14*). The existence of these problems indirectly drives much of the air pollution control program for the nation as a whole. While some measurements made in highway tunnels in the eastern states show emissions that are reasonably close to those expected given current emission inventory calculations (*15*), both experiments conducted in tunnels and remote sensing studies in California suggest that governmental emissions inventories historically have underestimated the actual VOC and CO emissions from the vehicle fleet operated in Los Angeles. In 1987, measurements made in Los Angeles in the Van Nuys tunnel suggested that the hot running CO and VOC exhaust emissions rates from in-use motor vehicles were approximately three times greater than those present in then-current governmental emissions inventory calculations (*16*, *17*). Subsequent remote sensing studies showed that high-emitting vehicles amounting to only 10% of the vehicle fleet are responsible for about 55% of the total CO emissions (*18*) and that cars and trucks that are more than 10 years old account for 58% of the total CO emissions (*1*). More recent studies of vehicular emissions in tunnels in northern California continue to show that the ratios of pollutant concentrations in the emissions from vehicles in actual use still differ from those predicted by governmental emissions inventories (*19*). Since air quality modeling emissions inventories for Los Angeles must continue to be corrected to reflect real-world emissions rates, it becomes very important to continue to monitor emissions from the Los Angeles in-use vehicle fleet through local

S0013-936X(97)00916-4 CCC: $15.00
Published on Web 06/05/1998

experiments conducted in highway tunnels.

Experimental Methods

Sampling Sites. Samples were collected at the Van Nuys Tunnel, where Sherman Way, a major east−west thoroughfare with three lanes of traffic in each direction, passes under the runway of the Van Nuys Airport. Samples were collected on September 21, 1993, from 0600 to 1000 PDT, during the morning traffic peak. Opposing traffic flow in the tunnel is separated by a wall. Eight open doorways through this wall exist at regular intervals between the two portals; the doorways account for only 0.3% of the interior surface of one bore of the tunnel. Samples were collected at a traffic turnout in the east-bound bore of the tunnel 147 m from the traffic entrance and 75 m from the exit of the tunnel. A second set of sampling equipment was sited outdoors directly above the location where the roadway enters the tunnel in order to measure the urban background pollutant concentrations already present in air entering the tunnel. A video camera was placed at the traffic turn-out within the tunnel to record the vehicles as they passed the sampling site. Vehicle counts, distributions by vehicle age and vehicle type, and estimates of vehicle speeds were obtained from the videotapes. Vehicle speed was estimated by timing vehicles over a known distance in the tunnel. The videotapes were processed by an expert traffic analyst, who determined the distribution of vehicles by age and type.

Sample Collection and Analysis. The methods used to collect and analyze samples taken at the Van Nuys Tunnel are the same as previously described for ambient atmospheric samples collected during the series of experiments of which this tunnel study forms a part (*8*−*12*), and thus they will only be briefly summarized here.

Internally electropolished stainless steel canisters were used to collect volatile organic compounds. The 6-L canisters were deployed to the field under high vacuum and used to collect both 4-h integrated and instantaneous grab samples. The concentrations of CO_2, CO, CH_4, individual organic compounds, and SF_6 were determined by a number of techniques including GC−MS, GC−FID (flame ionization detection), and GC−ECD (electron capture detection).

Aldehydes and other carbonyls were measured by collection on DNPH-impregnated C_{18} Sepak cartridges. Carbonyl compounds were trapped as their dinitrophenylhydrazones were extracted and analyzed by liquid chromatography (*9*).

High-volume dichotomous virtual impactors (*20*) operated at nominally 190 L min^{-1} were used to obtain enough organic material over the short sampling period to measure individual organic compounds in the particle and vapor phases. Fine particle collection occurred at a nominal flow rate of 170 L min^{-1} on 102 mm diameter prefired quartz fiber filters (Pallflex 2500 QAO). Directly downstream of the fine particle filter on the high-volume dichotomous sampler, polyurethane foam (PUF) cartridges were used to collect semivolatile organic compounds. GC−MS techniques were used to identify and quantify compounds from both the filter and polyurethane foam samples. A detailed description of the PUF materials and the extraction and analysis methods for both the filter and PUF samples by GC−MS are given elsewhere (*11*, *12*).

Low-volume particulate matter samplers were used to support the measurements needed to construct a material balance on the chemical composition of fine particles in the tunnel. Fine particles and total airborne particulate matter samples were collected by filtration along with certain inorganic gas-phase species that can be measured on chemically reactive filters. Fine particulate samples were collected downstream of a Teflon-coated AIHL (State of California Air and Industrial Hygiene Laboratory) cyclone separator (*21*). At the 34.7 L min^{-1} flow rate used during this experiment, the AIHL cyclone removed particles with a diameter larger than 1.6 μm. Samples were collected at flow rates of 10 and 4.9 L min^{-1} on two 47 mm diameter Teflon filters (Gelman Teflo) and at a flow rate of 10 L min^{-1} on one 47 mm diameter quartz fiber filter (Pallflex 2500 QAO) operated in parallel downstream of the cyclone separator. Particulate mass concentrations were measured gravimetrically by repeated weighings of the Teflon filters at 22 °C and 50% RH using a Mettler model M-55-A mechanical microbalance. The fine particle samples collected on one Teflon filter of each set were analyzed by X-ray fluorescence for 38 trace metals. Organic and elemental carbon concentrations were determined from the quartz fiber filters by the method of Birch and Cary (*22*). The quartz fiber filters (QFFs) were baked before use for at least 6 h at 550 °C to lower their carbon blanks. The denuder difference method employing two nylon filters (Gelman Nylasorb) operated downstream of the fine particle cyclone and cyclone/denuder combination, respectively, at a flow rate of 4.9 L min^{-1} each was used to measure gas-phase nitric and hydrochloric acids and fine particle nitrate and chloride (*23*, *24*). Extracts from the nylon filters and from the second fine particle Teflon filter of each set were analyzed by ion chromatography to measure nitrate, chloride, and sulfate concentrations. Additionally, atomic absorption spectrophotometry was used to measure particulate sodium and magnesium concentrations. Particle-phase ammonium ion collected on Teflon filters and gas-phase ammonia collected on oxalic acid-impregnated glass fiber filters downstream of a Teflon prefilter were measured by an indophenol colorimetric procedure (*25*). Ammonia emissions within the tunnel were found to be unexpectedly high and are reported in a separate paper where they can be discussed at length (*26*).

The integrity of the data was monitored through the collection, extraction, and analysis of the samples. Contaminants measured on field and laboratory blanks were excluded from the statement of emitted compounds. The normal carboxylic acids blank values measured on the polyurethane foam cartridges were present at a significant fraction of the ambient loadings; therefore, the ambient concentrations of these compounds could not be calculated, and the data are not included in this study. In all other cases, the blank levels were low compared to ambient concentrations, and the data presented here include these blank corrections.

Calculation of Emission Rates. Emission factors for traffic within a tunnel can be calculated per unit of fuel consumed (*1*) or per vehicle-kilometer-traveled (*16*, *27*). The method based on fuel consumption is particularly convenient for use in a tunnel study. In that case, the increase of CO_2, CO, and organic gases plus organic particulate matter within the tunnel directly matches the amount of carbon that was present in the fuel consumed, and emissions factors for each pollutant species per unit fuel consumed can be computed based on a carbon balance in the tunnel. Emissions rates computed per unit fuel burned based on this carbon balance are highly accurate; they are insensitive to uncertainties in air flow rates through the tunnel and are insensitive to the effect of any small air exchange between adjacent bores of the tunnel.

Results

The traffic through the tunnel was characterized from review of videotapes of the experiment. A total of 7060 vehicles were counted, 256 were identified as precatalyst light-duty vehicles (107 precatalyst light-duty vans and trucks and 149 precatalyst automobiles), 4546 were identified as catalyst-equipped automobiles, and 1936 were identified as catalyst-equipped light-duty trucks and vans. The age distribution

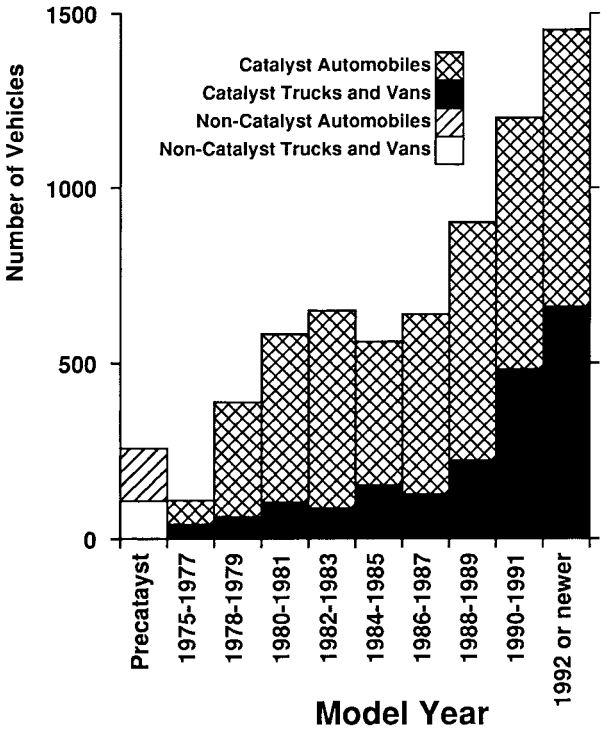

FIGURE 1. Model year distribution of light-duty vehicles passing through the Van Nuys Tunnel, 0600−1000 PDT, September 21, 1993.

for these light-duty vehicles is shown in Figure 1. Additionally, 12 diesel-powered light-duty vehicles, 277 heavy-duty vehicles, and 33 motorcycles were viewed on the videotapes. Of the 277 heavy-duty vehicles, 186 were identified as diesel-powered, and 91 were identified as gasoline-powered. The light-duty vehicle counts in Figure 1 show a decrease with increasing vehicle age, except for an excess of vehicles from model years between 1980 and 1983. The mean model year for gasoline-powered light-duty vehicles was 1986.4. The average light-duty vehicle being driven through the Van Nuys Tunnel was more than 7 years old during this experiment, older than the vehicle fleets typically seen in tunnel studies elsewhere (*15*, *19*) but very similar to the general distribution of vehicle traffic in Los Angeles as a whole (*1*). Since the 1990 model year there has been a significant increase in the fraction of the vehicle traffic contributed by light trucks (a category that includes minivans and sport utility vehicles). The average vehicle speed in the tunnel was approximately 64 km h^{-1} (40 mi h^{-1}).

Carbon Monoxide and Organic Vapor Emissions

Carbon monoxide emission rates of 130 g L^{-1} of gasoline-equivalent fuel and VOC emission rates of 9.1 g L^{-1} were measured for the vehicle fleet in the Van Nuys Tunnel during the current experiment. The data on CO, CO_2, and VOC concentrations needed to complete a carbon balance on the tunnel experiment are reported in ref *26*. These measured emissions rates are higher than reported for recent studies in highway tunnels in other cities. In the San Francisco Bay Area, 1994 emission rates of 4.2 g L^{-1} for VOC and 78.2 g L^{-1} for CO have been reported in the Caldecott Tunnel (*19*). However, the CO emissions in the Van Nuys tunnel in September 1993 amounting to 130 g L^{-1} are within the range of 108 ± 25 g L^{-1} for CO estimated for the hot stabilized exhaust emissions from the Los Angeles vehicle fleet in 1991 based on roadside remote sensing data (*1*). While the emissions rates measured in the Van Nuys Tunnel in the September 1993 experiment reported here are high, it is unlikely that this is due to experimental error. The emissions rates per unit of fuel burned are easily measured from a carbon balance that is insensitive to air flow and mixing conditions in the tunnel, and those emissions rates per unit fuel burned, while high, are within the range observed by roadside remote sensing studies of Los Angeles vehicle traffic in the early 1990s.

Particle Emissions

The ambient concentrations of the fine particle species measured inside and outside the tunnel are listed in Table 1. Reasonable agreement is seen between the mass concentrations determined by gravimetric weighings of Teflon filters versus the sum of the individual chemical species measured. On the basis of the difference between the ambient concentrations of particulate matter and gas-phase carbonaceous pollutants inside and outside the tunnel and the vehicle counts in the tunnel, the apparent fine particle emission rate from the vehicle traffic is calculated to be 491 ± 64 mg L^{-1}. The largest contributors to increased particle concentrations within the tunnel are organic compounds (141 ± 20 mg L^{-1}), elemental carbon (118 ± 13 mg L^{-1}), and ammonium nitrate (summing to 83 ± 6 mg L^{-1}). To the best of our knowledge, ammonium nitrate is not emitted directly from vehicle exhaust. Source test data show only traces of particulate nitrate from the vehicle tailpipe (*28*). Instead, substantial amounts of gas-phase NO_x are emitted, accompanied by 380 mg L^{-1} of gaseous ammonia during this experiment (*26*). These ammonia emissions are consistent with the performance of three-way catalyst-equipped vehicles that are running rich (*29*). The high primary ammonia

TABLE 1. Ambient Concentrations of Major Contributors to Fine[a] Particulate Matter Inside and Outside the Tunnel

component	tunnel concn (μg m^{-3})	background concn (μg m^{-3})	emission rate (mg L^{-1})
elemental carbon	11.1 ± 1.01	1.0 ± 0.47	117.5 ± 13.02
organic compounds[b]	21.7 ± 1.41	9.6 ± 1.02	141.4 ± 20.34
SiO_2	1.0 ± 0.09	0.9 ± 0.07	1.2 ± 1.33
Al_2O_3	0.4 ± 0.08	0.6 ± 0.08	0.0 ± 1.32
SO_4^{2-}	7.4 ± 0.21	7.4 ± 0.21	0.0 ± 3.47
Cl^-	0.8 ± 0.13	trace	9.2 ± 1.52
Mg^{2+}	0.6 ± 0.08	0.1 ± 0.01	5.1 ± 0.94
Na^+	1.0 ± 0.06	0.4 ± 0.02	7.6 ± 0.74
NO_3^-	10.8 ± 0.42	5.5 ± 0.21	61.9 ± 5.49
NH_4^+	4.3 ± 0.19	2.5 ± 0.11	21.0 ± 2.57
other trace metals	6.2 ± 1.33	7.0 ± 1.37	0.0 ± 22.32
sum of components	65.3 ± 2.26	35.0 ± 1.80	354.1 ± 33.8
gravimetric mass	68.2 ± 5.2	26.2 ± 1.8	490.9 ± 64.3

[a] Fine PM measured includes all particulate matter with $d_p \leq 1.6\ \mu$m. [b] Organic compound mass estimated as 1.4 × OC determined by thermal evolution and combustion analysis.

TABLE 2. Emission Rates for Individual Organic Compounds

compound	volatile organic compounds (mg L^{-1})	vapor-phase semivolatile compounds (μg L^{-1})	particulate organic compounds (μg L^{-1})	compound	volatile organic compounds (mg L^{-1})	vapor-phase semivolatile compounds (μg L^{-1})	particulate organic compounds (μg L^{-1})
			***n*-Alkanes**				
ethane	119			*n*-nonadecane		1298.8	60.5
propane	47			*n*-eicosane		745.1	48.9
n-butane	146			*n*-heneicosane		420.5	113.8
n-pentane	230			*n*-docosane		199.0	123.9
n-hexane	135			*n*-tricosane		91.0	164.5
n-heptane	8			*n*-tetracosane		19.6	229.2
n-octane	3			*n*-pentacosane		19.2	158.4
n-nonane	2			*n*-hexacosane		7.0	146.7
n-decane	1			*n*-heptacosane		2.9	104.0
n-undecane	1			*n*-octacosane		0.8	77.6
n-dodecane				*n*-nonacosane			128.3
n-tetradecane		415.8		*n*-triacontane			82.2
n-pentadecane		585.7		*n*-hentriacontane			93.4
n-hexadecane		2051.0		*n*-dotriacontane			48.4
n-heptadecane		2084.4	34.1	*n*-tricontane			33.7
n-octadecane		1661.8	55.6				
			Branched Alkanes				
2-methylpropane	14			3-methylheptane	60		
2-methylbutane	564			2,3-dimethylhexane	28		
2-methylpentane	242			2,4-dimethylhexane	45		
3-methylpentane	153			2,5-dimethylhexane	41		
2,3-dimethylbutane	68			2,2,4-trimethylpentane	208		
2-methylhexane	111			2,3,4-trimethylpentane	76		
3-methylhexane	119			2,4-dimethylheptane	5		
2,2-dimethylpentane	5			2,6-dimethylheptane	5		
2,4-dimethylpentane	70			norpristane		997.8	
2,3-dimethylpentane	122			pristane		1675.6	
3,3-dimethylpentane	5			phytane		1649.3	
2-methylheptane	47						
			Cyclic Alkanes				
cyclopentane	14			undecylcyclohexane		167.2	
cyclohexane	10			dodecylcyclohexane		154.9	
methylcyclohexane	23			tridecylcyclohexane		117.5	
methylcyclopentane	9			tetyradecylcyclohexane		132.0	
ethylcyclohexane	4			pentadecyclcyclohexane		149.6	
1-ethyl-4-methylcyclohexane	8			hexadecylcyclohexane		77.8	
nonylcyclohexane		48.2		heptadecylcyclohexane		33.4	
decylcyclohexane		149.8		octadecycyclohexane		7.2	
			Unresolved Complex Mixture				
unresolved complex mixture		231 000	113 000				
			Petroleum Biomarkers				
8β,13α-dimethyl-14β-*n*-butylpodocarpane		35.2		22,29,30-trisnorhopane			18.1
8β,13α-dimethyl-14β-[3′-methylbutyl]podocarpane		16.5		17α(*H*),21β(*H*)-29-norhopane			54.6
20*S*,13β(*H*),17α(*H*)-diacholestane			11.2	18α(*H*)-29-norneohopane			15.6
20*R*,13β(*H*),17α(*H*)-diacholestane			8.2	17α(*H*),21β(*H*)-hopane			82.0
20*R*,5α(*H*),14β(*H*),17β(*H*)-cholestane			11.4	22*S*,17α(*H*),21β(*H*)-30-homohopane			34.7
20*R*,5α(*H*),14α(*H*),17α(*H*)-cholestane			17.6	22*R*,17α(*H*),21β(*H*)-30-homohopane			23.3
20*R*+*S*,5α(*H*),14β(*H*),17β(*H*)-ergostane			22.3	22*S*,17α(*H*),21β(*H*)-30-bishomohopane			21.8
20*R*+*S*,5α(*H*),14β(*H*),17β(*H*)-sitostane			21.4	22*R*,17α(*H*),21β(*H*)-30-bishomohopane			14.0
22,29,30-trisnorneohopane			28.0				
			Gasoline Additives				
MTBE	155						
			Alkenes				
ethene	637			*trans*-2-pentene	40		
acetylene	486			3-methyl-1-butene	10		
propene	292			2-methyl-2-butene	50		
cis-2-butene	27			2-methyl-1-butene	35		
trans-2-butene	37			cyclopentene	6		
2-methylpropene	187			1-hexene	13		
1-pentene	27			2-hexenes	4		
cis-2-pentene	21						

TABLE 2. (Continued)

compound	volatile organic compounds (mg L^{-1})	vapor-phase semivolatile compounds (μg L^{-1})	particulate organic compounds (μg L^{-1})	compound	volatile organic compounds (mg L^{-1})	vapor-phase semivolatile compounds (μg L^{-1})	particulate organic compounds (μg L^{-1})
Aromatic Hydrocarbons							
benzene	382			C1-substituted anthracene		97.8	
toluene	748			C2-substituted MW 178 PAHs		385.7	
ethylbenzene	143			C3-substituted MW 178 PAHs		80.5	
n-propylbenzene	34			C4-substituted MW 178 PAHs		11.6	
isopropylbenzene	11			fluoranthene		390.5	3.6
o-xylene	200			acephenanthrylene		117.7	1.1
m/*p*-xylene	557			pyrene		512.3	6.2
o-ethyltoluene	56			C1-substituted MW 202 PAHs		159.3	7.8
m-ethyltoluene	67			C2-substituted MW 202 PAHs		28.7	5.9
p-ethyltoluene	149			C3-substituted MW 202 PAHs			4.9
1,2,3-trimethylbenzene	84			C4-substituted MW 202 PAHs			2.0
1,2,4-trimethylbenzene	219			benzo[*ghi*]fluoranthene		70.9	19.7
1,3,5-trimethylbenzene	77			cyclopenta[*cd*]pyrene		95.7	34.7
indane	40			benz[*a*]anthracene		15.5	20.9
1-methylindane	28			chrysene/triphenylene		18.7	23.8
4-methylindane	45			C1-substituted MW 226 PAHs			21.7
4,7-dimethylindane	7			C1-substituted MW 228 PAHs			39.9
naphthalene	326			C2-substituted MW 228 PAHs			17.9
2-methylnaphthalene	31			C3-substituted MW 228 PAHs			9.1
1-methylnaphthalene	25			benzo[*k*]fluoranthene			15.8
C2-substituted naphthalene		7778.0		benz[*e*]acephenanthrylene			16.1
C3-substituted naphthalene		3508.7		benzo[*j*]fluoranthene			4.9
C4-substituted naphthalene		1544.9		benzo[*e*]pyrene			21.7
acenaphthylene		1949.5		benzo[*a*]pyrene			18.3
fluorene		651.2		perylene			3.9
C1-substituted fluorene		364.8		C1-substituted MW 252 PAHs			19.6
C2-substituted fluorene		358.1		C2-substituted MW 252 PAHs			6.7
C3-substituted fluorene		173.9		indeno[123-*cd*]fluoranthene			10.4
phenanthrene		2456.1		indeno[123-*cd*]pyrene			30.6
anthracene		367.9		benzo[*ghi*]perylene			102.2
C1-substituted anthracene		632.3					
Substituted Aromatics							
benzaldehyde	20			fluorene-9-one		138.9	2.4
nitrobenzene		83.5		dibenzothiophene		55.3	8.8
benzyl alcohol		1618.1		benzothiazole		209.1	33.3
o-cresol		756.6		dibenzofuran		187.3	29.7
m+*p*-cresol		4449.1		antracene-9,10-dione		14.7	9.8
C2-substituted phenols		1973.1		phenalene-9-one		2.6	53.1
9-phenanthrol		205.7		benz[*de*]anthracene-7-one			12.7
indanone		670.3		benz[*a*]anthracene-7,12-dione			3.3
phthalan		17.6		benzo[*cd*]pyrene-6-one			54.0
phthalide		365.9					
Carbonyl Compounds							
formaldehyde	128			2-butanone	38		
acetaldehyde	29			crotonaldehyde	20		
hexanal	5			methylglyoxal	27		
nonanal	7						
Aromatic Acids							
benzoic acid		234.9		dehydroabietic acid			9.3
2-methylbenzoic acid		10.9		1,2-benzenedicarboxylic acid			566.9
3-methylbenzoic acid		126.8		1,3-benzenedicarboxylic acid			157.5
4-methylbenzoic acid		109.2		1,4-benzenedicarboxylic acid			135.5
2,6-dimethylbenzoic acid		35.4		4-methyl-1,2-benzene-dicarboxylic acid			211.1
2,5-dimethylbenzoic acid		197.2					
2,4-dimethylbenzoic acid		70.9		1,2,4-benzenetricarboxylic acid			281.3
3,5-dimethylbenzoic acid		90.0		1,2,3-benzenetricarboxylic acid			35.9
3,4-dimethylbenzoic acid		43.7		1,3,5-benzenetricarboxylic acid			5.5
naphthoic acid		30.2		1,2,4,5-benzenetetra-carboxylic acid			9.9
Other Acids							
palmitic acid			493.4	methylbutenedioic acid			41.6
stearic acid			302.9	pentanedioic acid			33.6
propanedioic acid			14.0	hexanedioic acid			7.5
butanedioic acid			97.3	nonanedioic acid			9.5
methylbutanedioic acid			23.5				

emissions then apparently lead to formation of fine particle ammonium nitrate inside the tunnel. If the secondary ammonium and nitrate formed are subtracted from the particle levels in the tunnel, the estimated primary fine particle emission rate in the tunnel equals 271 (sum of species method) to 408 mg L^{-1} (gravimetric mass difference method) ± 43.1−64.8 mg L^{-1}, respectively.

Fine particle emissions from vehicles include primary tailpipe particles from incomplete combustion in the engine as well as tire dust, brake dust, and re-entrained road dust. Road dust deposited on urban streets includes soil dust, organic material from vegetation, and deposited particulate emissions from vehicles, including tire dust and brake lining wear debris; dust from all these sources is continually deposited onto and re-entrained from street surfaces by passing vehicle traffic (*30*). The importance of fugitive soil dust entrained from the road surface under the conditions of the tunnel study as compared to tailpipe emissions can be judged by comparing the within-tunnel and outdoor concentrations of the inorganic elements aluminum and silicon that are used to track the soil dust component of road dust (*31*). X-ray fluorescence analysis of the fine particle samples shows that the levels of these two inorganic species are virtually identical inside and outside the tunnel, showing that fine particle soil dust resuspended by the vehicle traffic inside this particular tunnel is small. Organic chemical tracers, to be discussed shortly, can be used to set an upper bound on fine particle plant fragments and tire dust emissions within the tunnel.

Emissions of Individual Organic Compounds

Table 2 lists the emission rates of 221 organic compounds that are emitted from the vehicle fleet in the tunnel. Vapor-phase emissions measured by VOC canister and DNPH cartridge samplers are given in milligrams per liter of fuel consumed. Vapor-phase, semivolatile, and particle-phase organic compound emissions measured from PUF and filter samples are given in micrograms per liter of fuel burned. These emissions are grouped according to organic compound functionality, with the emission rates stated separately for vapor-phase, semivolatile, and particle-phase compounds. The emissions profile for the tunnel includes 64 aromatic hydrocarbons, 19 aromatic organic acids, 18 separate substituted aromatics, 31 normal alkanes, 23 branched alkanes, 16 cyclic alkanes, 17 petroleum biomarkers, 15 alkenes, 8 carbonyl compounds, 9 aliphatic organic acids, and the gasoline additive MTBE. These compound classes emitted from the vehicle fleet are measured in the VOC canister sampler and DNPH cartridges in amounts of 3.2 g L^{-1} of gasoline-equivalent fuel consumed for aromatics, 2.7 g L^{-1} for alkanes, 1.9 g L^{-1} for alkenes, 0.3 g L^{-1} for the carbonyls, and 0.2 g L^{-1} for MTBE. This corresponds to an emission rate of 8.3 g L^{-1} of identified compounds, leaving 0.8 g L^{-1} of total nonmethane organic compounds from the canister sampler that are not identified at the single compound level. Identified semivolatile organic compounds and the vapor-phase unresolved complex mixture (UCM) collected on the polyurethane foam but not measured from the canister sampler contribute less than 0.3 g L^{-1} to the organic gases.

Normal Alkanes. In addition to the low molecular weight *n*-alkanes present in gasoline and diesel fuel that are expected in the tunnel, emissions of particulate *n*-alkanes that are characteristic of plant waxes are also apparent. This plant wax signature is evident in the form of higher emission rates of odd-carbon number high molecular weight *n*-alkanes such as nonacosane (*n*-C_{29}) and hentriacontane (*n*-C_{31}) relative to even-carbon number alkanes of similar molecular weight and can be compared to the dominance of the odd-carbon number homologues in aerosol particles emitted from leaf surfaces in the southern California area (*32*, *33*). The excess of the C_{29}−C_{31} odd-carbon number *n*-alkanes seen within the tunnel over the smooth distribution of *n*-alkanes seen in crude oil (*34*) can be attributed to plant waxes entrained into the atmosphere from road dust (*30*). The amount by which the calculated emission rate, E_p, of the *n*-C_{29} alkane exceeds the *n*-C_{29} alkane contribution from petroleum provides one indication of the quantity of plant wax-containing particles in the tunnel atmosphere and is calculated as

$$\Delta E_p(n\text{-}C_{29})_{\text{attributable to plant waxes}} = E_p(n\text{-}C_{29})_{\text{total}} - \frac{E_p(n\text{-}C_{30}) + E_p(n\text{-}C_{28})}{2} \quad (1)$$

and a similar equation can be written for that portion of the emissions of the *n*-C_{31} alkane that is attributable to plant waxes using the emission rates of the *n*-C_{30} and the *n*-C_{32} alkanes. Using these techniques, the calculated emissions of excess *n*-C_{29} and *n*-C_{31} attributable to plant waxes are 48.4 and 28.1 μg L^{-1}, respectively. Using the emission rates of these compounds attributable to plant waxes and the composition of plant fragment particles shed from leaves in southern California (*31*), a rough estimate can be made of the emission rate of vegetative detritus within the tunnel that is created as tires pass over plant material on the road bed (*32*). The calculations show a range of contribution to particulate matter emissions in the tunnel due to plant fragments of 3.0−8.4 mg L^{-1}, which is about 2% or less of the gain in fine particle concentration in the tunnel.

Branched and Cyclic Alkanes. Two separate categories of branched and cyclic alkanes are apparent in the data presented in Table 2. High emission rates of low molecular weight alkanes (in the carbon number range from roughly C_5 to C_8) can be attributed to the presence of these compounds in gasoline. An additional class of semivolatile branched and cyclic parafins (in the carbon number range from roughly C_{18} to C_{22}) are emitted at a lower rate and can be attributed to the presence of these compounds in diesel fuels (*35*). In addition to these resolved branched and cyclic hydrocarbons, the emissions from vehicles contain unresolved branched and cyclic compounds, commonly called the unresolved complex mixture (UCM; *34*). The UCM is characteristic of petroleum and appears as a hump on GC traces underlying the resolved peaks of individual compounds. Large UCM humps are present in the polyurethane foam samples and the particulate matter samples collected inside the tunnel, accounting for 231 mg L^{-1} of semivolatile vapor-phase organics and 113 mg L^{-1} of particulate organics emissions. The UCM measured in the particle phase corresponds to approximately 80% of the total organic compound mass measured by combustion analysis of the particle samples.

Petroleum Biomarkers. Petroleum biomarkers are molecular fossils present in petroleum that reflect chemical structures originating from the microorganisms from which the petroleum deposits formed. These unique chemical structures can be used to trace the source of the organic matter from which the petroleum deposits were formed and also can be used to trace the presence of petroleum residues in the environment (*36*). Rogge et al. (*37*) and Schauer et al. (*31*) show that these petroleum biomarkers can be used to trace motor vehicle exhaust contributions to airborne particulate matter in the southern California atmosphere. Listed in Table 2 are the emission rates of 17 individual petroleum biomarkers seen in both the particulate matter and semivolatile organics samples.

Alkenes. The emission rates for 15 alkenes are given in Table 2. These compounds are among the most reactive in the atmosphere, leading to ozone formation (*38*), and for this reason fleet-average alkene emission rates are of considerable interest.

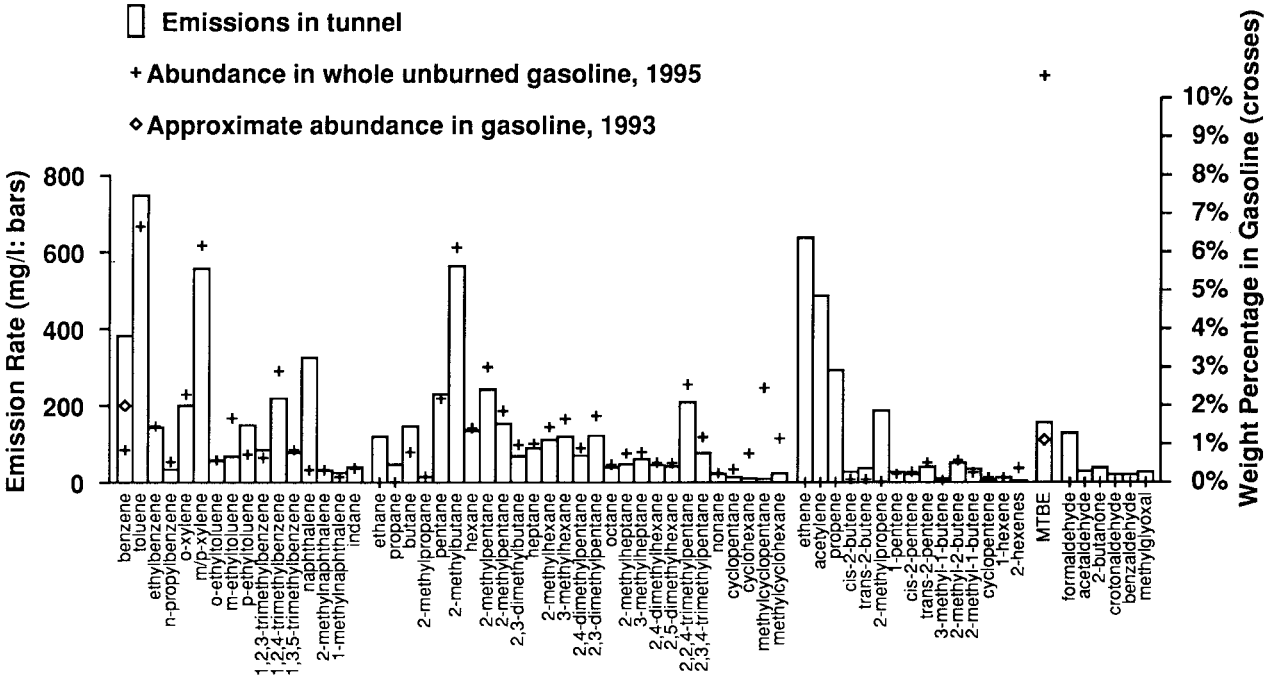

FIGURE 2. Compairson of the emissions rates of identified organic compounds within the Van Nuys Tunnel in September 1993 (bars) to the weight percentage of each compound in southern California gasoline (crosses, 1995 summer gasoline; diamonds, correction to conditions in summer 1993).

In Figure 2, the emission rates of volatile organic compounds within the tunnel are compared to the composition of average gasoline sold in southern California during the summer of 1995. The open bars represent the emission rate of the volatile organic compounds, and the crosses represent the weight percentage of that compound in gasoline. The gasoline sample was blended to represent a market share weighted average of the product of the six largest gasoline vendors in the Los Angeles area and was analyzed by gas chromatography to determine its chemical composition. While these two graphs need not necessarily track each other, there is a clear correlation for many organic compounds between the compound concentrations in gasoline and the relative compound emissions rates from the vehicle fleet inside the tunnel. During the interval between the summer 1993 tunnel study and the date of collection of the 1995 composite gasoline sample, new regulations mandated an increase in the oxygen content of gasoline from approximately 0.2% before the mandate (tunnel sample) to a minimum of 2% (gasoline sample), while reducing benzene in gasoline from approximately 2% to a maximum of 1%. Two percent oxygen in the fuel can be achieved by raising the MTBE content of gasoline to 11 wt %. The approximate levels of benzene and the oxygenated organic MTBE in southern California gasoline in 1993 before the latest reformulation are shown by the diamond symbols in Figure 2. From Figure 2, it is clear that those compounds for which the open bar substantially exceeds the corresponding cross are produced in the combustion process inside the engine. These include the light olefins, aldehydes, a portion of the benzene and possibly naphthalene.

Aromatic Hydrocarbons. Concern over the mutagenic and carcinogenic potential of aromatic hydrocarbons has led to efforts to understand their formation and atmospheric chemistry. The emission rates of 64 aromatic hydrocarbons measured in the vapor and particle phases are listed in Table 2. Aromatic compounds are present in trace amounts in petroleum products, including diesel fuel (*39*). Survival of these fuel components (*40*) as well as buildup of smaller molecules to form polycyclic aromatic hydrocarbons (PAHs) during high-temperature combustion and dealkylation of substituted aromatic compounds present in fuel are all mechanisms important in the emission of PAHs from vehicles.

Synthesis (buildup) of aromatic compounds from radical species during combustion will favor unsubstituted aromatic compounds over their alkylated homologues. Thus, an increase in unsubstituted over substituted aromatics relative to the composition of fuel should be diagnostic for the presence of benzene and naphthalene formed in combustion. This is clearly the case for benzene, as seen in Figure 2. Since the methyl-substituted naphthalenes in the tunnel samples are present at about their expected abundance relative to the composition of the gasoline pool, it appears that naphthalene is being synthesized in combustion as well.

Substituted Aromatic Compounds. Substituted aromatic compounds, including one nitro-aromatic and a variety of oxygenated aromatics are present in the emissions from vehicles in the Van Nuys Tunnel. The most prominent aromatic alcohols measured in vehicle exhaust include phenol, the cresols, and C_2-substituted phenols. Although phenol was detected in the Van Nuys tunnel, its concentration is not reported in Table 2 because of interference from its presence as one of the few contaminants in the benzene solvent used in extraction and concentration of the PUF samples. Cresols are commonly viewed as atmospheric reaction products of OH attack on toluene, which is one of the first steps in one aromatic oxidation pathway leading to secondary organic aerosol formation. The presence of significant direct emissions of cresols from vehicle exhaust means that it is possible for some aromatics to bypass the initial atmospheric attack of OH on toluene, thereby bypassing one of the rate-limiting steps in the oxidation pathway toward the formation of secondary organic aerosol from aromatic precursors. Analysis of the spatial distribution of cresols in the Los Angeles area atmosphere implies that primary emissions of these compounds dominate their atmospheric concentrations (*12*). For that reason, atmospheric oxidation of directly emitted cresols should be viewed as a potentially important competitor to atmospheric toluene oxidation as a source of secondary organic aerosol. Direct

emissions of vapor-phase cresols are seldom included in the vapor-phase organics profiles used to represent vehicle emissions within photochemical airshed models because as semivolatile compounds they are seldom measured even though their presence in vehicle exhaust has been reported previously (*41*).

The emissions rates of aromatic ketones, including monoketones and diketones, were measured within the Van Nuys Tunnel. Diketones in the atmosphere can come in part from atmospheric oxidation of primary aromatic hydrocarbons (*42*). The particular monoketones measured in the tunnel when found in the atmosphere are expected to be due entirely to primary emissions, because the precursor hydrocarbons for these compounds are not detected in the atmosphere (e.g., the 3-ring hydrocarbon structure that would constitute a precursor to phenalen-9-one).

Carbonyl Compounds. In a manner similar to the formation of light olefins and some unsubstituted aromatic compounds, Figure 2 shows that a variety of nonaromatic carbonyls also are formed during combustion. Methylglyoxal, which is one of the principal end-products of atmospheric aromatics oxidation also, is found in the direct emissions from motor vehicles, as shown in Table 2.

Alkanoic Acids. High molecular weight normal alkanoic acids, especially stearic (C_{18}) and palmitic (C_{16}) acids, are ubiquitous in atmospheric samples (*43*). Overall, the concentrations of most alkanoic acid homologues are about equal inside and outside the tunnel (within the error bounds on the quantification procedure) with palmitic and stearic acids being the only homologues that appear at substantially elevated concentrations inside the tunnel. High molecular weight *n*-alkanoic acids have been reported in the tailpipe emissions from vehicular sources (*37*, *44*) as well as in tire dust, brake lining wear dust, and paved road dust (*30*). Palmitic and stearic acids contributed over 50% of the mass concentration of the 27 *n*-alkanoic acids measured in road dust (*30*), with roughly twice the levels of palmitic acid when compared to stearic acid, a ratio very similar to that seen during the Van Nuys Tunnel experiment. Additionally, the relative concentration ratio within the tunnel between these two acids and the two normal alkane homologues attributed to plant waxes is similar to the concentration ratios seen in road dust samples collected in Los Angeles (*30*). In previously reported measurements of catalyst-equipped automobile exhaust composition (*37*), stearic and palmitic acids account for less than 15% of the total *n*-alkanoic acid emissions from the automobile tailpipe, with roughly four times as much palmitic acid as stearic acid. In heavy-duty diesel truck exhaust, these two homologues account for less than 20% of the total *n*-alkanoic acid emissions, with roughly twice as much palmitic as stearic acid (*47*). Stearic acids are a blending component that is added to tire rubber during manufacturing (*30*). In one tire dust sample analyzed to date, palmitic acid contributed 40% and stearic acid contributed 50% of the emissions of the *n*-alkanoic acids class (*30*). In brake lining wear particle samples analyzed to date, these two homologues together contribute about 30% of the emissions of *n*-alkanoic acids, with roughly equal contributions (*30*). Given the many contributing sources, it is not surprising that palmitic and stearic acids concentrations are elevated within the Van Nuys Tunnel. Their relative distribution in the tunnel is similar to that seen in the atmosphere (*45*), and indeed dry deposition of atmospheric aerosols may contribute these compounds to the roadway surface where they are reentrained into the atmosphere by vehicular traffic.

Aromatic Organic Acids. Emission rates for aromatic acids, including benzene carboxylic acids, benzene dicarboxylic acids, benzene tricarboxylic acids, and benzene tetracarboxylic acids are listed in Table 2. Previous reports have implicated vehicle traffic as a source of gas-phase benzoic acid (*46*) and particle-phase 1,2-benzenedicarboxylic acid and methyl-1,2-benzenedicarboxylic acid (*44*, *47*) to which we now add another 16 related compounds. Particle-phase polyfunctional acids in the Los Angeles atmosphere show spatial and seasonal trends that indicate significant formation by secondary reactions in the atmosphere involving gaseous precursors (*45*). It now appears that modeling of polyfunctional aromatic acids concentrations in the atmosphere will require consideration of both primary emissions and atmospheric photochemical oxidation processes.

The resin acid derivative dehydroabietic acid was quantified in the particle phase both inside and outside the tunnel. The particle-phase emission rate for this compound is calculated as 9.3 μg L^{-1}. This resin acid has been quantified in wood smoke (*48*), tire dust, and road dust particles (*30*). The presence of dehydroabietic acid in tire dust is probably due to the practice of adding conifer resins to the tire batch as an extender and softener. The source of dehydroabietic acid in road dust particles is most likely either from tire dust deposited onto the road or alternatively from the debris of coniferous plants ground up by passing traffic as part of the paved road dust mixture. Since woodsmoke is not a significant emission source during the summer in the Los Angeles area (*31*), an upper limit on the contribution of tire dust to the fine particle emission rate from vehicles and road dust can be estimated based on the ratio of dehydroabietic acid in tire dust to the emission rate of this compound inside the tunnel. Source test data for tire dust in southern California show 7970 μg of dehydroabietic acid per gram of tire dust sampled (*30*). On this basis, tire dust is estimated to contribute no more than 1.2 mg of fine particles per liter of fuel burned in the tunnel.

Discussion

The CO and vapor-phase organic compounds emissions rates of 130 g of CO and 9.1 g of VOC per liter of gasoline-equivalent fuel burned that were measured in 1993 in the Van Nuys tunnel were found to be higher than represented by governmental emissions inventories (e.g., EMFAC 7G; *49*) but are within the range of the 108 ± 25 g L^{-1} for CO reported by roadside remote sensing studies in Los Angeles (*1*). The detailed organic compound measurements made in the tunnel can be used to explore the possible cause of the higher VOC emission rates. One possibility is that an unusually large amount of unburned gasoline is either being emitted from the tailpipe or is leaking from vehicle fuel systems. Since the exhaust from properly functioning automobiles contains a large portion of unburned fuel components in any case, further enrichment has to be judged as an excess above the typical blend of burned and unburned exhaust hydrocarbons that is seen in laboratory-based tailpipe tests conducted on the vehicle fleets used for tracking compliance with emissions control regulations. As a rough approximation, we consider that the hydrocarbon composition of emissions in the tunnel is a linear combination of the auto exhaust characteristics seen in laboratory-based source tests plus an extra increment due to unburned whole gasoline. For each VOC species measured both in the tunnel and present in the source test database, an expression is written:

$$C_{i_{\text{tunnel}}} = \alpha C_{i_{\text{tailpipe}}} + (1 - \alpha) C_{i_{\text{fuel}}} + \delta(\alpha)_i \qquad (2)$$

where the C_i indicates the weight percent of species i in the tunnel, auto exhaust source test profile, and fuel composition data sets, and $\delta(\alpha)_i$ is the residual discrepancy between the tunnel data and a linear combination of the source profiles at a particular value of the unknown constant α. Using all VOC species appearing in the tunnel (except for benzene, butanes, and MTBE that have been affected by gasoline reformulation) plus the 1995 gasoline sample described in

Figure 2 and several auto source test databases, the value of α that minimizes the sum of the squared residual discrepancies was computed for several different automobile exhaust profiles. When the catalyst-equipped automobile exhaust profile of Harley et al. (*50*) is used to describe the vehicle tailpipe, the best estimate is that the tunnel atmosphere is dominated by auto tailpipe exhaust ($\alpha = 0.97$). When either the Exh801a vehicle profile published by Fujita et al. (*51*) or the noncatalyst auto exhaust profile of Harley et al. (*50*) are used, the best estimate is that the tunnel atmosphere is about 74−75% traditional tailpipe emissions plus 25−26% additional unburned gasoline (which of course could be either leaking from the fuel systems or coming from the tailpipes of poorly maintained cars). There is a very shallow minimum in the best choice of α, and thus a wide range of exhaust and fuel mixtures nearly reproduce the tunnel result.

The comprehensive vapor-phase organics data collected in the present study make it possible to explore the differences in the photochemical reactivity of the VOC emissions in the tunnel that would be estimated from the traditional VOC canister catch alone versus that seen when the additional species captured on the polyurethane foam and DNPH cartridge are added. The emission rates for the individual vapor-phase organic compounds were scaled according to their incremental reactivities on Carter's maximum incremental reactivity scale (*2*). Using this scale and summing contributions to reactivity for the individual organic compounds, the VOC canister sample accounted for 93% of the total reactivity measured by summing the VOC canister plus DNPH cartridge plus polyurethane foam sample for those compounds with known reactivity. Of those compounds not included in the VOC canister analysis, contributions from aldehydes and aromatic compounds contributed most of the additional reactivity.

The detailed information on fine particle composition in the tunnel likewise exposes interesting features of the emissions in the tunnel. The particles in this tunnel atmosphere during this particular experiment are almost entirely due to tailpipe emissions plus secondary ammonium nitrate formation. That is clear because the silicon, aluminum, dehydroabietic acid, and high molecular weight odd-carbon number alkanes concentrations set upper limits of a few milligrams per liter on the fine particle road dust, tire dust, and vegetative detritus that could be produced as fugitive emissions from the vehicle traffic, as explained earlier. The soot (EC) levels in the tunnel are higher than we initially expected relative to fine particle organics for the present case where diesel vehicles constitute 2.6% of the vehicle fleet in the tunnel. However, side calculations show that both the organic carbon and elemental carbon emission rates are within the range that could be achieved by this mix of vehicles, depending on the diesel engine technology used in the small fraction of the vehicles in the tunnel that have diesel engines. The EC emissions rates for the vehicle fleet in the air basin as a whole could be even higher since diesel vehicles accounted for 4.8% of the vehicle-kilometers-traveled in the South Coast Air Basin in 1993 (*52*). Knowing the organic chemical signature of a largely tailpipe emissions-dominated vehicle fleet, and particularly its petroleum biomarker content, it will be possible in future work to set an upper limit on the amount of primary tailpipe fine particulate organic matter that is present in the Los Angeles urban atmosphere by using organic molecular tracer techniques (*31*).

Acknowledgments

We thank Ed Ruth of UCLA for assistance with acquisition of the GC−MS data; Michael Hannigan and Claudine Butcher, who assisted with the field experiment; Kent Hoekman of Chevron Corporation, who assisted with analysis of the gasoline sample; William Ray, who assisted in vehicle identification; Eric and Daniel Grosjean for carbonyl compound analysis; and R. A. Rasmussen for VOC canister analysis. This research was supported by the Electric Power Research Institute under Agreement RP3189-03 and by the Caltech Center for Air Quality Analysis.

Literature Cited

(1) Singer, B. C.; Harley, R. A. *J. Air Waste Manage. Assoc.* **1996**, *46*, 581−593.
(2) Carter, W. P. L. *J. Air Waste Manage. Assoc.* **1994**, *44*, 881−899.
(3) *IARC Monographs*; World Health Organization, International Agency for Research on Cancer: Lyon, France, 1989; Vol. 46, pp 41−155.
(4) Odum, J. R.; Jungkamp, T. P. W.; Griffin, R. J.; Forstner, H. J. L.; Flagan, R. C.; Seinfeld, J. H. *Environ. Sci. Technol.* **1997**, *31*, 1890-1897.
(5) Lowenthal, D. H.; Zielinska, B.; Chow, J. C.; Watson, J. G.; Gautam, M.; Ferguson, D. H.; Neuroth, G. R.; Stevens, K. D. *Atmos. Environ.* **1994**, *28*, 731−743.
(6) Sagebiel, J. C.; Zielinska, B.; Pierson, W. R.; Gertler, A. W. *Atmos. Environ.* **1996**, *30*, 2287−2296.
(7) Zielinska, B.; Fung, K. K. *Sci. Total Environ.* **1994**, *147*, 281−288.
(8) Fraser, M. P.; Grosjean, D.; Grosjean, E.; Rasmussen, R. A.; Cass, G. R. *Environ. Sci. Technol.* **1996**, *30*, 1731−1743.
(9) Grosjean, E.; Grosjean, D.; Fraser, M. P.; Cass, G. R. *Environ. Sci. Technol.* **1996**, *30*, 2687−2703.
(10) Grosjean, E.; Grosjean, D.; Fraser, M. P.; Cass, G. R. *Environ. Sci. Technol.* **1996**, *30*, 2704−2714.
(11) Fraser, M. P.; Cass, G. R.; Simoneit, B. R. T.; Rasmussen, R. A. *Environ. Sci. Technol.* **1997**, *31*, 2356−2367.
(12) Fraser, M. P.; Cass, G. R.; Simoneit, B. R. T.; Rasmussen, R. A. *Environ. Sci. Technol.* **1998**, *32*, 1760−1770.
(13) National Research Council. *Rethinking the Ozone Problem in Urban and Regional Air Pollution*; National Academy Press: Washington, DC, 1991; 500 pp.
(14) Christoforou, C.; Salmon, L. G.; Hannigan, M. P.; Solomon, P. A.; Cass, G. R. *J. Air Waste Manage. Assoc.* Submitted for publication.
(15) Pierson, W. R.; Gertler, A. W.; Robinson, N. F.; Sagebiel, J. C.; Zielinska, B.; Bishop, G. A.; Stedman, D. H.; Zweidinger, R. B.; Ray, W. D. *Atmos. Environ.* **1996**, *30*, 2233−2256.
(16) Ingalls, M. N. *On-Road Vehicle Emission Factors from Measurements in a Los Angeles Area Tunnel*; Proceedings of the Air & Waste Management Association 82nd Annual Meeting, Anaheim, CA, 1989.
(17) Harley, R. A.; Russell, A. G.; McRae, G. J.; Cass, G. R.; Seinfeld, J. H. *Environ. Sci. Technol.* **1993**, *27*, 378−388.
(18) Lawson, D. R.; Groblicki, P. J.; Stedman, D. H.; Bishop, G. A.; Guenther, P. L. *J. Air Waste Manage. Assoc.* **1990**, *40*, 1096−1105.
(19) Kirchstetter, T. W.; Singer, B. C.; Harley, R. A.; Kendall, G. R.; Chan, W. *Environ. Sci. Technol.* **1996**, *30*, 661−670.
(20) Solomon, P. A.; Moyers, J. L.; Fletcher, R. A. *Aerosol Sci. Technol.* **1983**, *2*, 455-464.
(21) John, W.; Reischl, G. *J. Air Pollut. Control Assoc.* **1980**, *30*, 872−876.
(22) Birch, M. E.; Cary, R. A. *Aerosol Sci. Technol.* **1996**, *25*, 221−241.
(23) Solomon, P. A.; Larson, S. M.; Fall, T.; Cass, G. R. *Atmos. Environ.* **1988**, *22*, 1587−1594.
(24) Eldering, A.; Solomon, P. A.; Salmon, L. G.; Fall, T.; Cass, G. R. *Atmos. Environ.* **1991**, *25A*, 2091−2102.
(25) Bolleter, W. T.; Bushman, C. J.; Tidwell, P. W. *Anal. Chem.* **1961**, *33*, 592−594.
(26) Fraser, M. P.; Cass, G. R. *Environ. Sci. Technol.* **1998**, *32*, 1053−1057.
(27) Chang, T. Y.; Modzelewski, S. W.; Norbeck, J. M.; Pierson, W. R. *Atmos. Environ.* **1981**, *15*, 1011−1016.
(28) Hildemann, L. M.; Markowski, G. R.; Cass, G. R. *Environ. Sci. Technol.* **1991**, *25*, 744−759.
(29) Cadle, S. H.; Mulawa, P. A. *Environ. Sci. Technol.* **1980**, *14*, 718−723.
(30) Rogge, W. F.; Hildemann, L. M.; Mazurek, M. A.; Cass, G. R.; Simoneit, B. R. T.; *Environ. Sci. Technol.* **1993**, *27*, 1892−1904.
(31) Schauer, J. J.; Rogge, W. F.; Hildemann, L. M.; Mazurek, M. A.; Cass, G. R.; Simoneit, B. R. T. *Atmos. Environ.* **1996**, *30*, 3837−3855.
(32) Rogge, W. F.; Hildemann, L. M.; Mazurek, M. A.; Cass, G. R.; Simoneit, B. R. T. *Environ. Sci. Technol.* **1993**, *27*, 2700−2711.
(33) Hildemann, L. M.; Rogge, W. F.; Cass, G. R.; Mazurek, M. A.; Simoneit, B. R. T. *J. Geophys. Res.* **1996**, *101*, 19541−19549.

(34) Simoneit, B. R. T. *Int. J. Environ. Anal. Chem.* **1986**, *23*, 207−237.
(35) Zielinska, B.; Sagebiel, J. C.; Harshfield, G.; Gertler, A. W.; Pierson, W. R. *Atmos. Environ.* **1996**, *30*, 2269−2286.
(36) Peters, K. E.; Moldowan, J. M. *The Biomarker Guide*; Prentice-Hall: Englewood Cliffs, NJ, 1993; 363 pp.
(37) Rogge, W. F.; Hildemann, L. M.; Mazurek, M. A.; Cass, G. R.; Simoneit, B. R. T. *Environ. Sci. Technol.* **1993**, *27*, 636−651.
(38) Atkinson, R. *Atmos. Environ.* **1990**, *24A*, 1−41.
(39) Williams, P. T.; Bartle, K. D.; Andrews, G. E. *Fuel* **1986**, *65*, 1150−1158.
(40) Tancell, P. J.; Rhead, M. M.; Pemberton, R. D.; Braven, J. *Environ. Sci. Technol.* **1995**, *29*, 2871−2876.
(41) Mulawa, P. A.; Cadle, S. H. *Anal. Lett.* **1981**, *14*, 671−687.
(42) Jang, M. McDow, S. R. *Environ. Sci. Technol.* **1997**, *31*, 1046−1053.
(43) Simoneit, B. R. T.; Mazurek, M. A. *Atmos. Environ.* **1982**, *16*, 2139−2159.
(44) Simoneit, B. R. T. *Int. J. Environ. Anal. Chem.* **1985**, *23*, 203−233.
(45) Rogge, W. F.; Hildemann, L. M.; Mazurek, M. A.; Cass, G. R.; Simoneit, B. R. T. *Atmos. Environ.* **1993**, *27A*, 1309−1330.
(46) Kawamura, K.; Ng, L. L.; Kaplan, I. R. *Environ. Sci. Technol.* **1985**, *19*, 1082−1086.
(47) Kawamura, K.; Kaplan, I. R. *Environ. Sci. Technol.* **1987**, *21*, 105−110.
(48) Rogge, W. F.; Hildemann, L. M.; Mazurek, M. A.; Simoneit, B. R. T.; Cass, G. R. *Environ. Sci. Technol.* **1998**, *32*, 13−22.
(49) Heirigs, P.; Caretto, L. Sierra Research, Sacramento, CA, personal communication, 1997.
(50) Harley, R. A.; Hannigan, M. P.; Cass, G. R. *Environ. Sci. Technol.* **1992**, *26*, 2395-2408.
(51) Fujita, E. M.; Watson, J. G.; Chow, J. C.; Lu, Z. *Environ. Sci. Technol.* **1994**, *28*, 1633-1649.
(52) *1997 Air Quality Management Plan: Appendix III. Revised Attachment C: On-Road Mobile Emissions by Vehicle Class*; South Coast Air Quality Management District: Diamond Bar, CA, 1997.

Received for review October 20, 1997. Revised manuscript received March 9, 1998. Accepted March 23, 1998.

ES970916E